
Disentangled Unsupervised Skill Discovery for Efficient Hierarchical Reinforcement Learning

Anonymous Author(s)

Affiliation

Address

email

Abstract

1 A hallmark of intelligent agents is the ability to learn reusable skills purely from
2 unsupervised interaction with the environment. However, existing unsupervised
3 skill discovery methods often learn *entangled* skills where one skill variable si-
4 multaneously influences many entities in the environment, making downstream
5 skill chaining extremely challenging. We propose **Disentangled Unsupervised**
6 **Skill Discovery (DUSDi)**, a method for learning *disentangled skills* that can be
7 efficiently reused to solve downstream tasks. DUSDi decomposes skills into dis-
8 entangled components, where each skill component only affects one factor of the
9 state space. Importantly, these skill components can be **concurrently** composed
10 to generate low-level actions, and efficiently chained to tackle downstream tasks
11 through hierarchical Reinforcement Learning. DUSDi defines a novel mutual-
12 information-based objective to enforce disentanglement between the influences of
13 different skill components, and utilizes value factorization to optimize this objective
14 efficiently. Evaluated in a set of challenging environments, DUSDi successfully
15 learns disentangled skills, and significantly outperforms previous skill discovery
16 methods when it comes to applying the learned skills to solve downstream tasks¹.

17 1 Introduction

18 Reinforcement learning (RL) algorithms have achieved many successes in complex tasks, from
19 magnetic plasma control [10] to automobile racing [47]. However, applying existing RL algorithms
20 to every new task in a *tabula rasa* manner often results in low sample efficiency that limits RL’s
21 broader applicability. Unsupervised skill discovery holds the promise of improving the sample
22 efficiency of Reinforcement Learning, by learning a set of reusable skills through reward-free
23 interaction with the environment that can be later recombined to tackle multiple downstream tasks
24 more efficiently. In practice, prior unsupervised RL skills are represented as a policy that conditions
25 on a skill variable to generate diverse behaviors, and have led to successful and efficient learning of
26 downstream tasks when combined with skill fine-tuning or hierarchical RL skill selection [12, 22].

27 Despite prior successes, a common limitation of the skills learned by existing unsupervised RL
28 methods is that they are *entangled*: any change in the skill variable causes the agent to induce changes
29 in *multiple dimensions* of the state space simultaneously. Learning to use and recombine these
30 *entangled* skills can be extremely hard for an agent trying to solve downstream tasks, especially in
31 complex domains like multi-agent systems or household humanoid robots, where the agent needs to
32 concurrently change multiple independent dimensions of the state to complete the task. For example,
33 consider an agent learning to drive: if a single skill variable simultaneously changes the speed,
34 steering, and headlights of the car, it will be extremely challenging for the agent to learn how to

¹Website: <https://sites.google.com/view/dusdi>

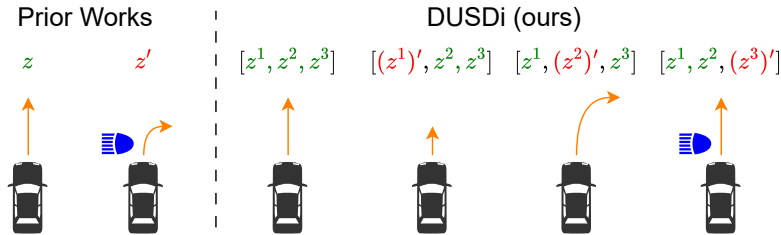


Figure 1: Consider an agent practicing driving skills by learning to control a car’s speed (length of orange arrow), steering (curvature of orange arrow), and headlights (blue symbol), **(Left)** previous unsupervised skill discovery methods learn *entangled* skills, where a change in the skill variable can cause all three environment factors to change **(Right)** DUSDi learns *disentangled skills* with concurrent components, where each skill component only affects one factor of the state space, enabling efficient downstream task learning with hierarchical RL.

35 turn on/off the headlights while keeping the car at the right speed and direction. In contrast, humans
 36 naturally have the ability to concurrently and independently adjust the car’s acceleration, steering,
 37 and headlights based on the car’s current speed, surroundings, and lighting conditions. In other words,
 38 humans learn *disentangled* skill components where each component only affects one or few state
 39 variables, and can be easily recombined into *compositional skills*.

40 In this work, we aim to create such a mechanism for artificial agents to learn disentangled skills
 41 that facilitate solving downstream tasks. We introduce Disentangled Unsupervised Skill Discovery
 42 (DUSDi), a novel method for unsupervised discovery of disentangled skills. A key insight of
 43 DUSDi is to take advantage of state factorization that is naturally available in unsupervised RL
 44 environments [12, 32, 16] (e.g. speed, direction, and lighting conditions of the car in the driving
 45 example; the state of different objects in a household environment). These factored state spaces
 46 provide a natural inductive bias we leverage for disentanglement: DUSDi decomposes skills into
 47 disentangled components, and encourages each skill component to affect only one state factor while
 48 discouraging it from affecting any other factors. To that end, DUSDi designs a novel intrinsic reward
 49 based on mutual information (MI) between disentangled skills and state factors: the learning agent
 50 receives high reward for 1) increasing the MI between a state factor and the skill component assigned
 51 to change it, and 2) for decreasing the MI between that skill component and all other state factors.

52 DUSDi introduces a set of technical innovations to efficiently optimize the proposed mutual infor-
 53 mation objective. Once the DUSDi skills are learned, they can be used as the low-level policy in a
 54 hierarchical reinforcement learning (HRL) setting to tackle downstream tasks. Compared to using
 55 entangled skills, a key benefit of using the disentangled DUSDi skills is that they guarantee more
 56 efficient exploration during downstream task learning and therefore often lead to significantly better
 57 performance. Furthermore, the structured skill space of DUSDi opens up additional possibilities to
 58 inject domain knowledge into the learning process to further improve downstream task learning.

59 DUSDi is easy to implement and can be integrated into any MI-based unsupervised skill discovery
 60 approach. In our experiments, we integrate DUSDi with DIAYN [12] and evaluate the performance
 61 on four domains: a 2D agent navigation domain, a DMC walker domain, a large-scale multi-agent
 62 particle domain, and a 3D realistic simulated robotics domain. Our experiments indicate that DUSDi
 63 can indeed learn disentangled skills, and significantly outperforms other Unsupervised Reinforcement
 64 Learning methods on solving complex downstream tasks with HRL.

65 2 Preliminaries

66 **Factored Markov Decision Process (f-MDP)** In this work, we consider unsupervised skill discov-
 67 ery in a reward-free Factored Markov Decision Process. Following Osband and Van Roy [30], we
 68 define a Factored Markov Decision Process by the tuple $\mathcal{M} = (\mathcal{S}, \mathcal{A}, \mathcal{P})$, where $\mathcal{S} = \mathcal{S}^1 \times \dots \times \mathcal{S}^N$
 69 is a factored state space with N factors such that each state $s \in \mathcal{S}$ consists of N state factors:
 70 $s = (s^1, \dots, s^N)$, $s^i \in \mathcal{S}^i$. \mathcal{A} is the action space, and \mathcal{P} is an unknown Markovian transition model,
 71 $\mathcal{S} \times \mathcal{A} \rightarrow \mathcal{S}$. Notice that a factored state space is often naturally available in domains used by
 72 prior works [12, 22, 32, 16, 8] as it can naturally represent environments with separate elements
 73 (e.g., objects) that can be changed independently. In domains with only image-based (unfactored)

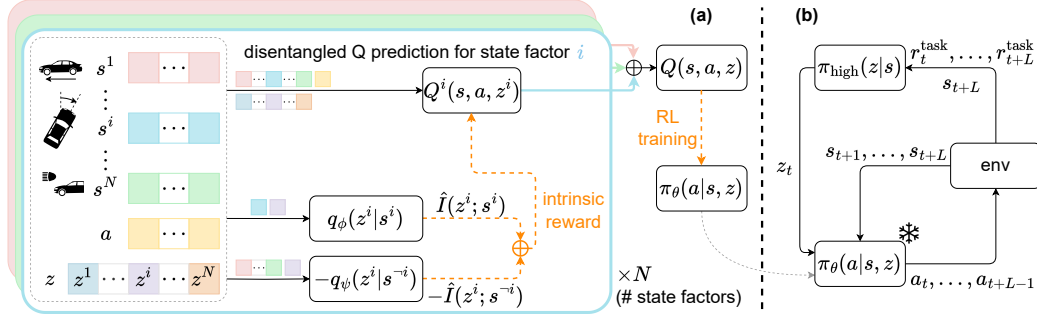


Figure 2: Two learning stages of DUSDi: **(a)** in *disentangled* skill learning stage, DUSDi creates a one-to-one mapping between state factors and skill components — each disentangled skill component z^i only influences state factor s^i . DUSDi designs a novel mutual-information-based intrinsic reward to enforce disentanglement and utilize Q -value decomposition to learn the skill policy π_θ efficiently. **(b)** in the task learning stage, the skill policy is used as a frozen low-level policy and a high-level policy π_{high} is learned to select skill z for every L steps, by maximizing the task reward r^{task} .

74 observations, a factored state space can be extracted using disentangled representation learning or
 75 object-centric representation learning methods [29, 18], which we empirically evaluated in Sec. 4.5.

76 **Mutual-Information-Based Skill Discovery** Mutual-information-based skill discovery methods,
 77 such as the paradigmatic DIAYN [12], specify the skills with a latent variable $z \in \mathcal{Z}$, and learns a
 78 skill-conditioned policy $\pi(a|s, z)$. The optimization objective these methods use to learn the skills
 79 is to maximize the mutual information (MI) between the state, s , and the skill latent variable, z :
 80 $I(\mathcal{S}; \mathcal{Z})$, which incentivizes the agent to reach diverse and distinguishable states. One popular way to
 81 determine the MI, $I(\mathcal{S}; \mathcal{Z})$, is to decompose it as $I(\mathcal{S}; \mathcal{Z}) = H(\mathcal{Z}) - H(\mathcal{Z} | \mathcal{S})$, where H denotes
 82 entropy. Since the skill variable is typically sampled from a fixed distribution, $H(\mathcal{Z})$ can be assumed
 83 constant: maximizing $I(\mathcal{S}; \mathcal{Z})$ is thus equivalent to minimizing $H(\mathcal{Z} | \mathcal{S})$. Following the definition
 84 of conditional entropy, $-H(\mathcal{Z} | \mathcal{S}) = \mathbb{E}_{s,z}[\log p(z|s)]$, DIAYN proposes to approximate $p(z|s)$ with
 85 a learned *discriminator* $q(z|s)$ that predicts the skill latent, z , given the state, s .

86 After discovering the skills, mutual-information-based methods apply them to learn downstream
 87 reward-supervised tasks. Many methods (e.g., DIAYN) adopt a hierarchical RL structure for this
 88 second phase, where the skill policy is used as a low-level “frozen” element, and a high-level policy
 89 $\pi_{\text{high}}(z|s)$ learns to sequentially activate skill z based on observations. The high-level policy is trained
 90 to maximize the provided task reward, \mathcal{R} , with \mathcal{Z} as the action space.

91 3 Learning Disentangled Skills with DUSDi

92 DUSDi acts in two phases: in the first phase, DUSDi learns disentangled skills without external
 93 reward (Sec. 3.1). The key to DUSDi’s success is to encourage disentanglement between different
 94 skill components through a novel learning objective that restricts the effect of each disentangled skill
 95 component to independent factors. In the second phase, DUSDi learns to perform downstream tasks
 96 with explicit reward supervision using a Hierarchical RL architecture, achieving higher returns than
 97 methods with entangled skills (Sec. 3.3). In practice, learning disentangled skills in environments
 98 with many factors can be challenging. To address this challenge, we introduce improvements to
 99 DUSDi’s first phase based on Q -function decomposition (Sec. 3.2). We present the entire DUSDi
 100 pipeline in Fig. 2, and the pseudo-code in Appendix A.

101 3.1 Disentangled Skill Spaces and Learning Objective

102 DUSDi aims to create disentangled skill components that can be easily recombined to solve down-
 103 stream tasks. To that end, DUSDi proposes a novel factorization of the latent skill conditioning
 104 variable, z , into N independent disentangled components such that the latent space \mathcal{Z} becomes
 105 $\mathcal{Z} = \mathcal{Z}^1 \times \dots \times \mathcal{Z}^N$. We equate N to the number of state factors and consider $z^i \in \mathcal{Z}^i$ the disentan-
 106 gled skill component that affects state factor i . The skill policy $\pi(a|s, z)$ takes in $z \in \mathcal{Z}$, which is a
 107 composition of the skill components.

108 While, in principle, the factored latent space could be discrete or continuous, without loss of generality
 109 we assume in this paper that the skill space is discrete, which also leads to more clarity in the
 110 presentation. We can then assume that each disentangled component z^i takes the form of an integer,
 111 $z^i \in [1, k]$, resulting in a compositional skill, z , with the form of a N -dimensional multi-categorical
 112 vector with k^N possible values. During skill training, we independently sample each disentangled
 113 component z^i from a fixed uniform distribution $p(z^i)$, similar to Eysenbach et al. [12].

114 Given this factored skill space, our goal is to learn a skill policy network, $\pi_\theta : \mathcal{S} \times \mathcal{Z} \mapsto \mathcal{A}$,
 115 such that each disentangled component \mathcal{Z}^i affects and only affects the value of a state factor,
 116 \mathcal{S}^i . For each disentangled component and state factor pair $(\mathcal{Z}^i, \mathcal{S}^i)$, we encourage diverse and
 117 distinguishable behaviors by maximizing their mutual information $I(\mathcal{S}^i; \mathcal{Z}^i)$. While this objective
 118 enables a disentanglement skill component to affect the corresponding factor, it does not restrict the
 119 component from affecting other factors. This is undesirable since the resulting skill components
 120 would still be entangled in their effects. To prevent that, we propose to ensure that each skill
 121 component, \mathcal{Z}^i , minimally affects the rest of the state factors, \mathcal{S}^{-i} , where \mathcal{S}^{-i} denotes the subspace
 122 formed by all other state factor spaces except \mathcal{S}^i : $\mathcal{S}^1 \times \dots \times \mathcal{S}^{i-1} \times \mathcal{S}^{i+1} \times \dots \times \mathcal{S}^N$. Specifically,
 123 we incorporate an entanglement penalty to minimize, $I(\mathcal{S}^{-i}; \mathcal{Z}^i)$, which corresponds to the mutual
 124 information between a skill component and all other state factors that it should not affect.

125 Formally, the skill policy aims to maximize the following objective:

$$\mathcal{J}(\theta) = \sum_{i=1}^N I(\mathcal{S}^i; \mathcal{Z}^i) - \lambda I(\mathcal{S}^{-i}; \mathcal{Z}^i), \quad (1)$$

126 where $\lambda < 1$ is a hyperparameter that controls the importance of the entanglement penalty relative to
 127 the skill-factor association. We restrict λ to be smaller than one for the following reason: in some
 128 environments, due to intrinsic dynamical dependencies between state factors themselves, controlling
 129 a state factor, \mathcal{S}^i , has to introduce some association between \mathcal{Z}^i and other factors in \mathcal{S}^{-i} , e.g., when
 130 controlling an object whose manipulation requires the agent to use other objects as tools. In these
 131 cases, as the policy learns to maximize the MI between a skill and a factor, $I(\mathcal{S}^i; \mathcal{Z}^i)$, the MI with
 132 other factors, $I(\mathcal{S}^{-i}; \mathcal{Z}^i)$, may also increase. For these cases, the use of $\lambda < 1$ will ensure that the
 133 entanglement penalty does not overpower the association reward, and the policy is still incentivized
 134 to learn disentangled skill components that change \mathcal{S}^i distinguishably while introducing minimal
 135 changes on other factors. In practice, we simply set $\lambda = 0.1$ in all our experiments.

136 **Optimizing DUSDi’s Objective:** Directly maximizing the objective in Eq. 1 is intractable. Alter-
 137 natively, we propose to approximate the objective using a variational lower bound of the mutual
 138 information [1]:

$$I(\mathcal{S}^i; \mathcal{Z}^i) = H(\mathcal{Z}^i) - H(\mathcal{Z}^i | \mathcal{S}^i) \geq C + \mathbb{E}_{z,s} \log q_\phi^i(z^i | s^i), \quad (2)$$

139 where C represents the constant value of $H(\mathcal{Z}^i)$, the entropy of the prior distribution over the skill
 140 latent variable, which does not change during training, and q_ϕ^i is a variational distribution.

141 Similarly, we can approximate the MI in the entanglement penalty by:

$$I(\mathcal{S}^{-i}; \mathcal{Z}^i) \geq C + \mathbb{E}_{z,s} \log q_\psi^i(z^i | s^{-i}), \quad (3)$$

142 where q_ψ^i is another variational distribution. Importantly, when these q approximations perfectly
 143 recover the posterior distribution of z^i , we obtain equality in Eq. 2 and Eq. 3. We implement the
 144 variational distributions, q_ϕ and q_ψ , as neural network discriminators mapping input state factor(s) to
 145 the predicted disentangled component values, z^i .

146 To optimize $\mathcal{J}(\theta)$, we alternate between two steps: 1) performing variational inference to train the
 147 discriminators q_ϕ^i and q_ψ^i through gradient ascent, and 2) using q_ϕ^i and q_ψ^i to learn a disentangled skill
 148 policy π_θ through RL by maximizing the following intrinsic reward approximating Eq. 1:

$$r_z(s, a) \triangleq \sum_{i=1}^N q_\phi^i(z^i | s^i) - \lambda q_\psi^i(z^i | s^{-i}) \quad (4)$$

149 Notice that because of the negative sign in front of the entanglement penalty, $-q_\psi^i(z^i | s^{-i})$, we are no
 150 longer optimizing a variational lower bound on $\mathcal{J}(\theta)$. Despite that, we found empirically that our

151 optimization procedure works well as an approximation for $\mathcal{J}(\theta)$, possibly because both q_ϕ^i and q_ψ^i
 152 quite accurately approximate the underlying simple categorical distribution.

153 Interestingly, the decomposed nature of our intrinsic reward allows a convenient avenue for shaping
 154 skill behaviors based on domain knowledge. In particular, we can restrict a state factor s^i to only
 155 take certain values by constraining $q_\phi^i(z^i|s^i)$ accordingly. While not the main focus of this work, we
 156 briefly explore this further optimization enabled by DUSDi in Appendix I.

157 3.2 Accelerating Skill Learning through Q Decomposition

158 When using reinforcement learning (RL) to optimize the intrinsic reward function defined in Eq. 4,
 159 standard RL algorithms treat the reward function as a black box and learn a single value function
 160 from the mixture of intrinsic reward terms. While this approach may be sufficient for environments
 161 with few state factors, doing so for complex environments with many state factors (large N) often
 162 leads to suboptimal solutions. A key reason is that the mixture of $2N$ reward terms leads inevitably
 163 to high variance in the reward, making the value of the Q function oscillate. Furthermore, the sum of
 164 reward terms obscures information about each term’s value, which hinders credit assignment.

165 DUSDi overcomes this issue by leveraging the fact that the intrinsic reward function in Eq. 4 is
 166 a linear sum over terms associated with each disentangled component. Thanks to the linearity of
 167 expectation, we can decompose the Q function into N disentangled Q functions as follows:

$$Q_\pi(s, a, z) = \sum_{i=1}^N Q^i(s, a, z) \quad (5)$$

168 where Q^i represents each disentangled Q function, one for each disentangled component. We prove
 169 Eq. 5 in Appendix H. The disentangled Q functions can be then updated only with their corresponding
 170 intrinsic reward terms, $r^i \triangleq q_\phi^i(z^i|s^i) - \lambda q_\psi^i(z^i|s^{-i})$. During policy learning, we sum all disentangled
 171 Q functions together to recover the global critic, Q_π , as shown in Fig. 2 (a), top. Compared to learning
 172 Q_π directly from all $2N$ reward terms, learning disentangled Q functions significantly reduces reward
 173 variance, allowing Q_π to converge faster and more stably.

174 Notice that the decomposed Q function provides a convenient way to inject domain prior and improve
 175 training efficiency. This can be done by constraining each decomposed Q function to only attend to a
 176 (often small) subset of the state and skill factors that matter, which we leave for future work.

177 3.3 Downstream Task Learning

178 Similar to Eysenbach et al. [12], in DUSDi we utilize hierarchical RL to solve reward-supervised
 179 downstream tasks with the discovered skills, as depicted in Fig.2 (b). The skill policy, $\pi_\theta : \mathcal{S} \times \mathcal{Z} \rightarrow$
 180 \mathcal{A} , acts as the low-level policy and is kept constant while a high-level policy, $\pi_{\text{high}} : \mathcal{S} \rightarrow \mathcal{Z}$, learns
 181 to select which skill to execute for L steps using the skill latent variable, z . Thus, the skill latent
 182 conditioning space, \mathcal{Z} , acts as the action space of the high-level policy, π_{high} . As extensively evaluated
 183 in our experiments, without any additional “ingredient”, performing downstream task learning in the
 184 action space formed by DUSDi skills often results in significantly superior performance compared to
 185 an action space formed by entangled skills. We show that the superior performance of DUSDi can be
 186 explained by **more efficient exploration** when using the DUSDi skills for hierarchical RL, which we
 187 elaborate on in Appendix B.

188 Depending on the nature of the downstream tasks, we can often take further advantage of the
 189 disentangled skills learned by DUSDi through leveraging its structure. One such scenario is when
 190 the downstream task has a composite reward function consisting of multiple terms. Previous works
 191 [15, 42] have shown that when the causal dependencies from action dimensions to reward terms are
 192 available (e.g., the reward for speed only depends on actions that affect speed), one can use Causal
 193 Policy Gradient (CPG) to decompose the policy update (e.g., only the “speed actions” get updated
 194 by the speed reward) and greatly improve sample efficiency, especially when the dependencies are
 195 sparse. In downstream task learning, with an action space (of the high-level policy) consisting of
 196 the skills learned by DUSDi, we have a convenient way of applying causal policy gradient, where
 197 the causal dependencies between the action dimensions (i.e., skill components) and reward terms
 198 are often sparse and can be easily obtained by examining the state factor that a skill component is
 199 associated with, which we evaluate empirically in Sec. 4.6.

Table 1: Evaluation of skill disentanglement based on the DCI metric, shown as mean and standard deviation across skill policies trained with 3 random seeds.

	2D GUNNER		MULTI-PARTICLE		IGIBSON	
	DUSDi (ours)	DIAYN-MC	DUSDi (ours)	DIAYN-MC	DUSDi (ours)	DIAYN-MC
Disentanglement (\uparrow)	0.864 \pm 0.018	0.016 \pm 0.002	0.705 \pm 0.037	0.002 \pm 0.000	0.833 \pm 0.022	0.017 \pm 0.006
Completeness (\uparrow)	0.864 \pm 0.017	0.024 \pm 0.004	0.750 \pm 0.041	0.003 \pm 0.000	0.834 \pm 0.021	0.019 \pm 0.005
Informativeness (\uparrow)	0.897 \pm 0.012	0.821 \pm 0.010	0.849 \pm 0.052	0.791 \pm 0.032	0.854 \pm 0.006	0.752 \pm 0.015

200 4 Experimental Evaluation

201 In the evaluation of DUSDi, we aim to answer the following questions: **Q1**: Are skills learned by
 202 DUSDi truly disentangled (Sec. 4.2)? **Q2**: Can Q-decomposition improve skill learning efficiency
 203 (Sec. 4.3)? **Q3**: Do our disentangled skills perform better when solving downstream tasks compared
 204 to other unsupervised reinforcement learning methods (Sec. 4.4)? **Q4**: Can DUSDi be extended to
 205 image observation environments (Sec.4.5)? **Q5**: Can we leverage the structured skill space of DUSDi
 206 to further improve downstream task learning efficiency (Sec.4.6)?

207 4.1 Evaluation Environments

208 Previous works [12, 31, 32, 40, 21] extensively rely on standard RL environments such as DMC [43]
 209 and OpenAI Fetch [3] to evaluate unsupervised RL methods. However, unlike previous unsupervised
 210 skill discovery methods, DUSDi focuses on learning a set of disentangled skill components that
 211 can be concurrently executed and re-combined to complete downstream tasks. As such, it only
 212 makes sense to examine the performance of DUSDi in challenging tasks that require concurrent
 213 control of many environment entities (e.g. multi-agent systems, complex household robots). Previous
 214 environments lack this property: in DMC for example, while the state and action space can be very
 215 complex, the predominant downstream tasks are just to move the center-of-mass of the agent to
 216 different places. In such cases, there is no need for concurrent skill components, and therefore we
 217 do not expect large gains from using DUSDi’s disentangled skills. Nevertheless, we include an
 218 evaluation on the **DMC-Walker** [43] environment to demonstrate that our method is also applicable
 219 to those environments, but focus the majority of our evaluation on environments that DUSDi is
 220 designed for, including **2D Gunner**, **Multi-Particle** [28], and **iGibson** [24].

221 The 2D gunner is a relatively simple domain, where a point agent can navigate inside a continuous
 222 2D plane, collecting ammo and shooting at targets. Multi-Particle is a multi-agent domain modified
 223 based on [28]. In this domain, a centralized controller simultaneously controls 10 heterogenous
 224 point-mass agents to interact with 10 stations, where each agent can only interact with a specific
 225 station. We evaluate in this domain to test the scalability of our methods to a large number of state
 226 factors. iGibson [24] is a realistic simulated robotics domain, where a mobile manipulator can
 227 navigate in a room, inspect the room using its head camera, and interact with electric appliances in
 228 the room by pointing a remote control to them and switching them on/off. We evaluate in this domain
 229 to examine whether our method can handle home-like environments with complex dynamics. We
 230 provide visualizations and additional information about each of the environments in Appendix C.

231 4.2 Evaluating Skill Disentanglement

232 First, we examine whether the skills learned by DUSDi are truly disentangled (**Q1**) using the DCI
 233 metric proposed by Eastwood and Williams [11]. The DCI metric consists of three terms, namely
 234 **disentanglement**, **completeness**, and **informativeness**, explained in detail in Appendix F. We
 235 compare against **DIAYN-MC** (Multi-channel DIAYN) that uses the same skill representation as
 236 DUSDi but optimizes the DIAYN objective of $I(\mathcal{S}; \mathcal{Z})$, and show results in Table 1. Unsurprisingly,
 237 DUSDi significantly outperforms DIAYN-MC, especially on Disentanglement and Completeness,
 238 across all three environments. These results indicate that DUSDi learns truly disentangled skills,
 239 enabling efficient downstream task learning, as we will show in Sec. 4.4. Qualitatively, we showcase
 240 some of the learned skills in <https://sites.google.com/view/dusdi>.

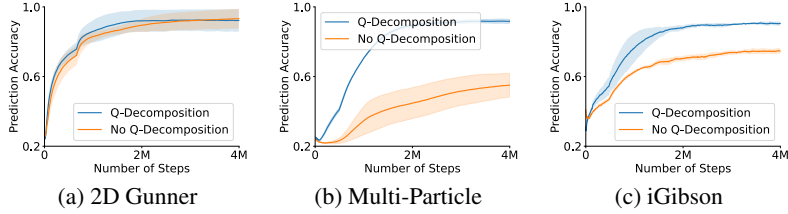


Figure 3: Evaluation of the effect of Q-decomposition in skill learning. The plots depict the mean and standard deviation of accuracy (\uparrow) when predicting the skill component z^i based on the state factor s^i , computed across 3 training processes. The higher prediction accuracy indicates that the policy learns to control more state factors in more distinguishable ways, leading to more efficient downstream task learning.

241 4.3 Evaluating Skill Learning Efficiency with Q-decomposition

242 To examine the importance of Q-decomposition (**Q2**), we measure the performance of optimizing the
 243 DUSDi objective during skill learning with and without a decomposed Q network. We compare the
 244 classification accuracy of the skill discriminators $q_\phi^i(z^i|s^i)$, averaged over all skill channels, which
 245 indicates progress towards discovering diverse and distinguishable skills, with higher accuracy being
 246 better. We depict our results in Fig. 3. We observe that Q-decomposition has a similar performance to
 247 the regular Q network in the simplest 2D gunner domain, but significantly outperforms the regular Q
 248 network in domains with more state factors (Multi-Particle) and more complex dynamics (iGibson),
 249 suggesting that Q-decomposition is necessary for scaling towards complex domains.

250 4.4 Evaluating Downstream Task Learning

251 The promise of DUSDi is to incorporate disentanglement into skills so that the skills can be effectively
 252 used in downstream task learning. Therefore, the most critical evaluation of our work focuses on
 253 comparing the performance of different unsupervised RL methods on task learning (**Q3**). We
 254 compare against existing state-of-the-art unsupervised reinforcement learning algorithms, including
 255 **DIAYN** [12], **CIC** [22], **CSD** [32], **METRA** [33], **ICM** [34], **RND** [4], **ELDEN** [16], and **Vanilla**
 256 **RL** [13], where these baselines are further explained in Appendix E.

257 Similar to the evaluation setting in the URLB benchmark [21], we allow each method to train for
 258 4 million steps without access to reward (i.e., pretraining phase) before the reward is revealed to
 259 the agent and the downstream learning takes place. During the pre-training phase, all methods use
 260 soft actor-critic (SAC) [13] to optimize the intrinsic reward. For all skill discovery methods (i.e.,
 261 DUSDi, DIAYN, CIC, CSD, METRA), a skill-conditioned policy, $\pi_\theta(a|s, z)$, is learned during the
 262 pretraining phase. During downstream learning, the skill network is fixed, whereas an upper policy,
 263 $\pi_{\text{high}}(z|s)$, is trained using proximal policy optimization (PPO) [39] to optimize the task reward.
 264 Similar to previous works [12, 40], we omit proprioceptive states from the MI optimization for all
 265 skill discovery methods. For exploration methods (i.e., RND, ICM, ELDEN), a policy $\pi_\theta(a|s)$ is
 266 learned during the pretraining phase on intrinsic reward and fine-tuned using the task reward during
 267 the downstream learning phase. The hyperparameters are specified in Appendix G.

268 We evaluate all methods in four environments and 13 downstream tasks, detailed in Appendix D. The
 269 results are depicted in Fig. 4. As expected, DUSDi performs similarly to previous unsupervised RL
 270 methods in the DMC walker environment due to the simplicity in terms of its downstream objectives
 271 (all related to center-of-mass locomotion), but significantly outperforms all previous methods on
 272 domains where downstream tasks require coordinative control of multiple state factors. The most
 273 crucial comparison is between DUSDi and DIAYN. DIAYN is a special case of DUSDi where
 274 there is only one state factor (consisting of the entire state) and one skill component. Therefore
 275 comparing against DIAYN offers a straightforward examination of the effect of disentangled skills
 276 for downstream task learning. DUSDi significantly outperforms DIAYN in all downstream tasks,
 277 demonstrating the effectiveness of using disentangled skills. In general, we found exploration-based
 278 methods to be less capable than skill discovery methods, possibly due to their lack of temporal
 279 abstraction. CIC performs very poorly, likely because the CIC objective does not explicitly encourage
 280 distinguishable skills and instead generates the intrinsic reward solely based on state entropy, making it
 281 very hard for the upper policy to select the right skill. This result again shows the importance of having
 282 a proper skill representation. DUSDi also outperforms CSD and METRA on most downstream tasks,
 283 especially on the more complex and high-dimensional domains, like Multi-Particle. This superiority is

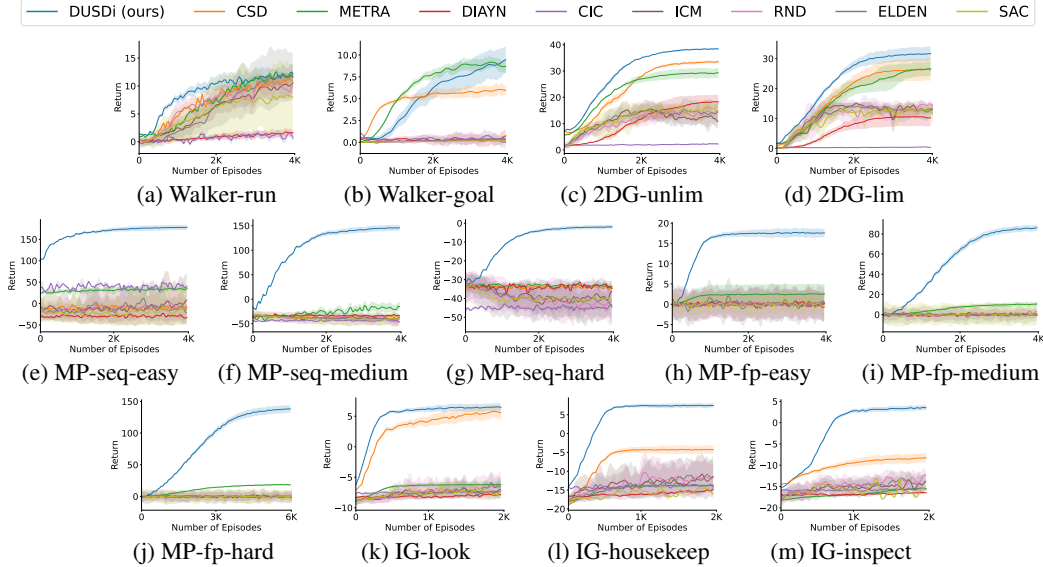


Figure 4: Training curves of DUSDi and baselines on multiple downstream tasks (reward supervised second phase). The plots depict the mean and standard deviation of the return of each method over 3 random seeds. DUSDi outperforms all baselines that learn entangled skills, converging faster and to higher returns.

284 perhaps surprising considering that in our experiments, DUSDi only relies on the simple DIAYN-style
 285 intrinsic reward for skill discovery, but further demonstrates the importance of learning a disentangled
 286 skill space. It is important to notice that many techniques proposed to improve skill discovery quality
 287 (e.g., Baumli et al. [2], Zhao et al. [50]), can be seamlessly incorporated into DUSDi. Therefore, we
 288 expect our method to perform even better as new advances are made in unsupervised skill discovery.

289 4.5 Extending DUSDi to Image Space

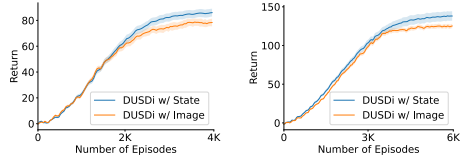
290 Although this paper primarily focuses on applying DUSDi to factored state space, we can straightforwardly
 291 extend it to image space through existing works in factored / object-centric representation
 292 learning [27, 18, 46, 26, 48] (Q4). We empirically illustrate this capability in the Multi-Particle envi-
 293 ronment, where we replace the low-dimensional state observation with 64×64 image observations.
 294 Specifically, we first pretrain an object-centric encoder following Yang et al. [48], and then use our
 295 method on top of the extracted representation to learn disentangled skills. Hence, essentially, the
 296 skill policy uses images as observation. As shown in Fig. 5, when learning from image observation,
 297 DUSDi achieves similar performance to learning from state space, whereas the baseline methods are
 298 unable to learn these two tasks even when learning from the low-dimensional state space as in Fig. 4.

299 4.6 Leveraging Structure of DUSDi Skills

300 While DUSDi can already learn downstream tasks quite efficiently, it is possible to further improve
 301 the sample efficiency of downstream task learning through leveraging the structured skill space of
 302 DUSDi (Q5), as described in the second paragraph of Sec.3.3. Specifically, we apply Causal Policy
 303 Gradient [15] to the Multi-Particle domain, where the causal dependencies between state factors and
 304 reward terms are easy to identify. We present our results in Fig. 6, where the sample efficiency of
 305 downstream task learning is greatly improved thanks to the structured skill space of DUSDi.

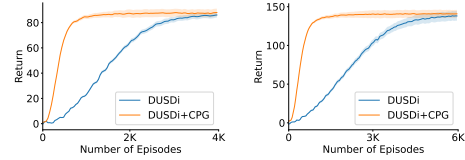
306 5 Related Work

307 **Unsupervised Skill Discovery** In unsupervised skill discovery, the goal of an agent is to learn
 308 task-agnostic skills without external rewards. To learn such skills, previous methods propose various
 309 forms of intrinsic reward: (1) maximizing the mutual information between visited states and the skill
 310 variables [12, 40, 5, 22], (2) maximizing the traveled distance along the direction specified by the
 311 skill variables [31–33], (3) learning to reach a diverse set of goals [45, 37, 35]. These skills can be



(a) MP-fp-medium (b) MP-fp-hard

Figure 5: Performance of DUSDi with image observations on two multi-particle downstream tasks over three random seeds. With the help of disentangled representation learning, DUSDi effectively learns skills based only on image observations and leverages the skills to solve challenging downstream tasks where baseline methods fail.



(a) MP-fp-medium (b) MP-fp-hard

Figure 6: Performance of DUSDi in two multi-particle downstream tasks when combined with Causal Policy Gradient (CPG, orange). The disentangled skills of DUSDi provide opportunities for leverage structure and speed up downstream task learning, greatly improving the sample efficiency when learning downstream tasks.

312 used to boost the sample efficiency of downstream task learning, for example, (1) using hierarchical
 313 RL where a high-level policy learns to select which skill to execute [12], or (2) using the skill policy
 314 to initialize the task solving policy and then fine-tuning it [22].

315 **State Space Factorization in RL** In RL, there is a long history of leveraging state factorization,
 316 including learning a world model between state factors for planning [20, 44], augmenting data [36],
 317 and providing intrinsic rewards [38, 16]. Relevant to our work are skill discovery methods that
 318 learn to either reach a goal for each controllable object [17, 8] or achieve interactions between a
 319 pair of specified objects [7]. Though these methods achieve disentanglement by influencing one or
 320 a pair of objects during a skill, they do not apply to tasks that require controlling multiple objects
 321 simultaneously, like driving where we need to control the car’s speed and heading directions at the
 322 same time. In contrast, our method can combine disentangled skill components into concurrent skills
 323 [9] to solve a wide range of tasks.

324 **Disentanglement in Skill Learning** There are a few works investigating disentanglement in un-
 325 supervised skill discovery. Lee et al. [23] consider a special case of disentangled skills — for a
 326 multi-arm robot, learning independent skills for each arm. However, they rely on manually factored
 327 action spaces which is an assumption that often limits the behavior of the agent. Kim et al. [19]
 328 encourage the disentanglement between different dimensions of the skill variable by regularizing it
 329 with β -VAE objective [14], but Locatello et al. [25] point out such regularization is impossible to
 330 achieve disentanglement. To learn disentangled skills, Song et al. [41] learns a decoder from skill
 331 variables to state trajectories and their generation factors, which is then used to train the skill policy
 332 through imitation learning. However, their training of the decoder requires pre-collected trajectories
 333 and corresponding generation factors, whereas our method is fully unsupervised with no expert data.

334 6 Conclusion

335 We present DUSDi, an unsupervised skill discovery method for learning disentangled skills by lever-
 336 aging the factorization of the state space. DUSDi designs a skill space that exploits the factorization
 337 of the state space and learns a skill-conditioned policy where each sub-skill affects only one state
 338 factor. DUSDi enforces disentanglement through an intrinsic reward based on mutual information,
 339 and shows superior performance on a set of downstream tasks with naturally factored state spaces
 340 compared to baselines and state-of-the-art unsupervised RL methods.

341 One limitation of DUSDi is the assumption of access to a factored state space. While a factored state
 342 space is naturally available in many existing RL environments, and can be extracted from images
 343 as we have shown in our experiment (Sec. 4.5), we believe that future advances in disentangled
 344 representation learning will greatly broaden the applicability of DUSDi. Secondly, DUSDi primarily
 345 focuses on learning a structured skill space for more efficient downstream learning, and its exploration
 346 capability during skill learning is largely determined by the specific algorithm used to optimize for
 347 our mutual information objective. While we used DIAYN [12] in this work due to its simplicity,
 348 it would be interesting to examine extending the idea of learning disentangled skills to other skill
 349 discovery methods, e.g., Zhao et al. [50], Laskin et al. [22], including those that are not based on
 350 mutual information [32, 49].

References

- 351
- 352 [1] David Barber and Felix Agakov. Information maximization in noisy channels: A variational
353 approach. *Advances in Neural Information Processing Systems*, 16, 2003.
- 354 [2] Kate Baumli, David Warde-Farley, Steven Hansen, and Volodymyr Mnih. Relative variational
355 intrinsic control. In *Proceedings of the AAAI conference on artificial intelligence*, volume 35,
356 pages 6732–6740, 2021.
- 357 [3] Greg Brockman, Vicki Cheung, Ludwig Pettersson, Jonas Schneider, John Schulman, Jie Tang,
358 and Wojciech Zaremba. Openai gym. *arXiv preprint arXiv:1606.01540*, 2016.
- 359 [4] Yuri Burda, Harrison Edwards, Amos Storkey, and Oleg Klimov. Exploration by random
360 network distillation, 2018.
- 361 [5] Víctor Campos, Alexander Trott, Caiming Xiong, Richard Socher, Xavier Giró-i Nieto, and
362 Jordi Torres. Explore, discover and learn: Unsupervised discovery of state-covering skills. In
363 *International Conference on Machine Learning*, pages 1317–1327. PMLR, 2020.
- 364 [6] Jongwook Choi, Archit Sharma, Honglak Lee, Sergey Levine, and Shixiang Shane Gu. Varia-
365 tional empowerment as representation learning for goal-based reinforcement learning. *arXiv*
366 *preprint arXiv:2106.01404*, 2021.
- 367 [7] Jongwook Choi, Sungtae Lee, Xinyu Wang, Sungryull Sohn, and Honglak Lee. Unsupervised
368 object interaction learning with counterfactual dynamics models. In *Workshop on Reincarnating*
369 *Reinforcement Learning at ICLR 2023*, 2023.
- 370 [8] Caleb Chuck, Kevin Black, Aditya Arjun, Yuke Zhu, and Scott Niekum. Granger-causal
371 hierarchical skill discovery. *arXiv preprint arXiv:2306.09509*, 2023.
- 372 [9] Cédric Colas, Tristan Karch, Olivier Sigaud, and Pierre-Yves Oudeyer. Autotelic agents with
373 intrinsically motivated goal-conditioned reinforcement learning: a short survey, 2022.
- 374 [10] Jonas Degraeve, Federico Felici, Jonas Buchli, Michael Neunert, Brendan Tracey, Francesco
375 Carpanese, Timo Ewalds, Roland Hafner, Abbas Abdolmaleki, Diego de Las Casas, et al.
376 Magnetic control of tokamak plasmas through deep reinforcement learning. *Nature*, 602(7897):
377 414–419, 2022.
- 378 [11] Cian Eastwood and Christopher KI Williams. A framework for the quantitative evaluation of
379 disentangled representations. In *International conference on learning representations*, 2018.
- 380 [12] Benjamin Eysenbach, Abhishek Gupta, Julian Ibarz, and Sergey Levine. Diversity is all you
381 need: Learning skills without a reward function. *arXiv preprint arXiv:1802.06070*, 2018.
- 382 [13] Tuomas Haarnoja, Aurick Zhou, Pieter Abbeel, and Sergey Levine. Soft actor-critic: Off-
383 policy maximum entropy deep reinforcement learning with a stochastic actor. In *International*
384 *conference on machine learning*, pages 1861–1870. PMLR, 2018.
- 385 [14] Irina Higgins, Loic Matthey, Arka Pal, Christopher Burgess, Xavier Glorot, Matthew Botvinick,
386 Shakir Mohamed, and Alexander Lerchner. beta-vae: Learning basic visual concepts with a
387 constrained variational framework. In *International conference on learning representations*,
388 2016.
- 389 [15] Jiaheng Hu, Peter Stone, and Roberto Martín-Martín. Causal policy gradient for whole-body
390 mobile manipulation. *arXiv preprint arXiv:2305.04866*, 2023.
- 391 [16] Jiaheng Hu, Zizhao Wang, Peter Stone, and Roberto Martin-Martin. Elden: Exploration via
392 local dependencies. *arXiv preprint arXiv:2310.08702*, 2023.
- 393 [17] Xing Hu, Rui Zhang, Ke Tang, Jiaming Guo, Qi Yi, Ruizhi Chen, Zidong Du, Ling Li, Qi Guo,
394 Yunji Chen, et al. Causality-driven hierarchical structure discovery for reinforcement learning.
395 *Advances in Neural Information Processing Systems*, 35:20064–20076, 2022.
- 396 [18] Jindong Jiang, Fei Deng, Gautam Singh, and Sungjin Ahn. Object-centric slot diffusion. *arXiv*
397 *preprint arXiv:2303.10834*, 2023.

- 398 [19] Jaekyeom Kim, Seohong Park, and Gunhee Kim. Unsupervised skill discovery with bottleneck
399 option learning. *arXiv preprint arXiv:2106.14305*, 2021.
- 400 [20] Thomas Kipf, Elise Van der Pol, and Max Welling. Contrastive learning of structured world
401 models. *arXiv preprint arXiv:1911.12247*, 2019.
- 402 [21] Michael Laskin, Denis Yarats, Hao Liu, Kimin Lee, Albert Zhan, Kevin Lu, Catherine Cang,
403 Lerrel Pinto, and Pieter Abbeel. *Urlb: Unsupervised reinforcement learning benchmark*, 2021.
- 404 [22] Michael Laskin, Hao Liu, Xue Bin Peng, Denis Yarats, Aravind Rajeswaran, and Pieter
405 Abbeel. *Cic: Contrastive intrinsic control for unsupervised skill discovery*. *arXiv preprint*
406 *arXiv:2202.00161*, 2022.
- 407 [23] Youngwoon Lee, Jingyun Yang, and Joseph J Lim. Learning to coordinate manipulation skills
408 via skill behavior diversification. In *International conference on learning representations*, 2019.
- 409 [24] Chengshu Li, Fei Xia, Roberto Martín-Martín, Michael Lingelbach, Sanjana Srivastava, Bokui
410 Shen, Kent Vainio, Cem Gokmen, Gokul Dharan, Tanish Jain, Andrey Kurenkov, C. Karen
411 Liu, Hyowon Gweon, Jiajun Wu, Li Fei-Fei, and Silvio Savarese. *igibson 2.0: Object-centric*
412 *simulation for robot learning of everyday household tasks*, 2021.
- 413 [25] Francesco Locatello, Stefan Bauer, Mario Lucic, Gunnar Raetsch, Sylvain Gelly, Bernhard
414 Schölkopf, and Olivier Bachem. Challenging common assumptions in the unsupervised learning
415 of disentangled representations. In *international conference on machine learning*, pages 4114–
416 4124. PMLR, 2019.
- 417 [26] Francesco Locatello, Ben Poole, Gunnar Rätsch, Bernhard Schölkopf, Olivier Bachem, and
418 Michael Tschannen. Weakly-supervised disentanglement without compromises. In *International*
419 *Conference on Machine Learning*, pages 6348–6359. PMLR, 2020.
- 420 [27] Francesco Locatello, Dirk Weissenborn, Thomas Unterthiner, Aravindh Mahendran, Georg
421 Heigold, Jakob Uszkoreit, Alexey Dosovitskiy, and Thomas Kipf. Object-centric learning with
422 slot attention, 2020.
- 423 [28] Ryan Lowe, Yi Wu, Aviv Tamar, Jean Harb, Pieter Abbeel, and Igor Mordatch. Multi-agent
424 actor-critic for mixed cooperative-competitive environments. *Neural Information Processing*
425 *Systems (NIPS)*, 2017.
- 426 [29] Sindy Löwe, Phillip Lippe, Francesco Locatello, and Max Welling. Rotating features for object
427 discovery. *arXiv preprint arXiv:2306.00600*, 2023.
- 428 [30] Ian Osband and Benjamin Van Roy. Near-optimal reinforcement learning in factored mdps.
429 *Advances in Neural Information Processing Systems*, 27, 2014.
- 430 [31] Seohong Park, Jongwook Choi, Jaekyeom Kim, Honglak Lee, and Gunhee Kim. Lipschitz-
431 constrained unsupervised skill discovery. *arXiv preprint arXiv:2202.00914*, 2022.
- 432 [32] Seohong Park, Kimin Lee, Youngwoon Lee, and Pieter Abbeel. Controllability-aware unsuper-
433 vised skill discovery. *arXiv preprint arXiv:2302.05103*, 2023.
- 434 [33] Seohong Park, Oleh Rybkin, and Sergey Levine. Metra: Scalable unsupervised rl with metric-
435 aware abstraction. *arXiv preprint arXiv:2310.08887*, 2023.
- 436 [34] Deepak Pathak, Pulkrit Agrawal, Alexei A. Efros, and Trevor Darrell. Curiosity-driven explo-
437 ration by self-supervised prediction, 2017.
- 438 [35] Silviu Pitis, Harris Chan, Stephen Zhao, Bradly Stadie, and Jimmy Ba. Maximum entropy gain
439 exploration for long horizon multi-goal reinforcement learning. In *International Conference on*
440 *Machine Learning*, pages 7750–7761. PMLR, 2020.
- 441 [36] Silviu Pitis, Elliot Creager, and Animesh Garg. Counterfactual data augmentation using locally
442 factored dynamics. *Advances in Neural Information Processing Systems*, 33:3976–3990, 2020.

- 443 [37] Vitchyr H Pong, Murtaza Dalal, Steven Lin, Ashvin Nair, Shikhar Bahl, and Sergey
444 Levine. Skew-fit: State-covering self-supervised reinforcement learning. *arXiv preprint*
445 *arXiv:1903.03698*, 2019.
- 446 [38] Cansu Sancaktar, Sebastian Blaes, and Georg Martius. Curious exploration via structured
447 world models yields zero-shot object manipulation. *Advances in Neural Information Processing*
448 *Systems*, 35:24170–24183, 2022.
- 449 [39] John Schulman, Filip Wolski, Prafulla Dhariwal, Alec Radford, and Oleg Klimov. Proximal
450 policy optimization algorithms, 2017.
- 451 [40] Archit Sharma, Shixiang Gu, Sergey Levine, Vikash Kumar, and Karol Hausman. Dynamics-
452 aware unsupervised discovery of skills. *arXiv preprint arXiv:1907.01657*, 2019.
- 453 [41] Wonil Song, Sangryul Jeon, Hyesong Choi, Kwanghoon Sohn, and Dongbo Min. Learning
454 disentangled skills for hierarchical reinforcement learning through trajectory autoencoder with
455 weak labels. *Expert Systems with Applications*, page 120625, 2023.
- 456 [42] Thomas Spooner, Nelson Vadori, and Sumitra Ganesh. Factored policy gradients: Leveraging
457 structure for efficient learning in momdps, 2021.
- 458 [43] Yuval Tassa, Yotam Doron, Alistair Muldal, Tom Erez, Yazhe Li, Diego de Las Casas, David
459 Budden, Abbas Abdolmaleki, Josh Merel, Andrew Lefrancq, Timothy Lillicrap, and Martin
460 Riedmiller. Deepmind control suite, 2018.
- 461 [44] Zizhao Wang, Xuesu Xiao, Zifan Xu, Yuke Zhu, and Peter Stone. Causal dynamics learning for
462 task-independent state abstraction. *arXiv preprint arXiv:2206.13452*, 2022.
- 463 [45] David Warde-Farley, Tom Van de Wiele, Tejas Kulkarni, Catalin Ionescu, Steven Hansen, and
464 Volodymyr Mnih. Unsupervised control through non-parametric discriminative rewards. *arXiv*
465 *preprint arXiv:1811.11359*, 2018.
- 466 [46] Ziyi Wu, Nikita Dvornik, Klaus Greff, Thomas Kipf, and Animesh Garg. Slotformer: Unsuper-
467 vised visual dynamics simulation with object-centric models. *arXiv preprint arXiv:2210.05861*,
468 2022.
- 469 [47] Peter R Wurman, Samuel Barrett, Kenta Kawamoto, James MacGlashan, Kaushik Subramanian,
470 Thomas J Walsh, Roberto Capobianco, Alisa Devlic, Franziska Eckert, Florian Fuchs, et al.
471 Outracing champion gran turismo drivers with deep reinforcement learning. *Nature*, 602(7896):
472 223–228, 2022.
- 473 [48] Mengyue Yang, Furui Liu, Zhitang Chen, Xinwei Shen, Jianye Hao, and Jun Wang. Causalvae:
474 Disentangled representation learning via neural structural causal models. In *Proceedings of the*
475 *IEEE/CVF conference on computer vision and pattern recognition*, pages 9593–9602, 2021.
- 476 [49] Rushuai Yang, Chenjia Bai, Hongyi Guo, Siyuan Li, Bin Zhao, Zhen Wang, Peng Liu, and
477 Xuelong Li. Behavior contrastive learning for unsupervised skill discovery, 2023.
- 478 [50] Rui Zhao, Yang Gao, Pieter Abbeel, Volker Tresp, and Wei Xu. Mutual information state
479 intrinsic control. *arXiv preprint arXiv:2103.08107*, 2021.

480 **A Pseudo-code for DUSDi Skill Learning**

Algorithm 1 DUSDi Skill Learning

- 1: Initialize skill policy π_θ , discriminators q_ϕ^i, q_ψ^i and value function Q^i for each state factor \mathcal{S}^i .
 - 2: **for** each skill training episode **do**
 - 3: Sample skill $z \sim p(z)$.
 - 4: Collect state transitions with actions from $\pi_\theta(a|s, z)$.
 - 5: Sample a batch of (s, a, z) from the replay buffer.
 - 6: **for** $i = 1, \dots, N$ **do**
 - 7: Update $q_\phi^i(z^i|s^i)$ and $q_\psi^i(z^i|s^{-i})$ with discrimination losses.
 - 8: Update $Q^i(s, a, z)$ with reward r^i using SAC.
 - 9: **end for**
 - 10: Update π_θ with $Q = \sum_{i=1}^N Q^i$ using SAC.
 - 11: **end for**
-

481 **B Entangled vs. disentangled components for Policy Learning**

482 Compared to entangled skills, the advantages of using disentangled components mainly reside in
 483 an easier exploration in the skill space. For skill spaces of equivalent capacity, the DIAYN latent
 484 skill variable is a *single* integer between 1 and k^N , and the DUSDi skill variable is a N -dimensional
 485 vector with each dimension representing a disentangled component with k possible values. In this
 486 section, we analyze the benefits and search complexity of DUSDi’s space over DIAYN’s for two main
 487 cases: when there are no dynamical dependencies between state factors (optimal case for disentangled
 488 components) and where there are intrinsic dependencies between state factors.

489 **State Factors without Dynamical Dependencies:** In this case, for DIAYN to find the correct
 490 skill to execute at the current time step, in the worst case, it needs to iterate through all skills,
 491 resulting in 1-step exploration sample-efficiency of $O(k^N)$. In contrast, for DUSDi, as disentangled
 492 components are independent of each other, with one skill trial, the agent can simultaneously observe
 493 the effects of setting each disentangled component as $\mathcal{Z}^i = z^i$. Hence, for an intelligent agent, to
 494 understand the effects of each disentangled component at the current state, it only needs to sweep
 495 through each disentangled component space with k trials (e.g., setting all disentangled components
 496 $\mathcal{Z}^i = 1, \dots, k$). After that, as the effects of each disentangled component are independent, by
 497 compositing disentangled components in novel ways, the agent has the ability to imagine the effects
 498 of all skills, leading to $O(k)$ exploration efficiency.

499 **State Factors with Dynamical Dependencies:** When there are dynamical dependencies, we denote
 500 PA^i as *parent* indices of state factors that \mathcal{S}^i depends on, e.g., when moving a mouse (\mathcal{S}^i), $\mathcal{S}^{\text{PA}^i}$
 501 denotes the hand. In such cases, the effect of \mathcal{Z}^i is conditioned on the value of $\mathcal{Z}^{\text{PA}^i}$, and we
 502 need to iterate through all $(\mathcal{Z}^i, \mathcal{Z}^{\text{PA}^i})$ pairs to observe all possible influences on \mathcal{S}^i . As a result,
 503 the exploration is constrained by the state factor with the largest number of parents. Denoting
 504 $|\text{PA}^i|$ as the number of parent factors for \mathcal{S}^i , the exploration sample-efficiency is $O(k^{1+\max_i |\text{PA}^i|})$.
 505 We can see that the $O(k)$ efficiency when there is no dynamical dependencies is a special case
 506 of $\max_i |\text{PA}^i| = 0$. Despite lower efficiency than $O(k)$, in many environments, the dynamics of
 507 each state factor only depend on a small number of other factors, i.e., $\max_i |\text{PA}^i| \ll N$. Hence,
 508 exploration with disentangled components is still more sample-efficient than using entangled skills.

509 **C Environment Details**

510 We test DUSDi on four environments, where a visualization of each of the environments is presented
 511 in Fig. 7.

512 **2D Gunner:** Shown in Fig. 7 (a), the blue star marks the position of the agent, the blue line marks
 513 its shooting direction, the red diamond marks ammo location, and the orange cross marks the target

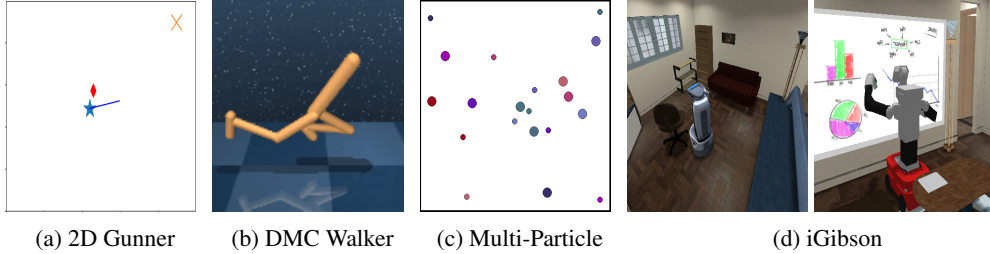


Figure 7: Environments Visualization

514 position. The agent has a 7-dimensional observation space, consisting of 3 state factors: [Agent
515 Position, Ammo State, Target State]. The action is 5-dimensional, 2 for agent movement, 2 for ammo
516 pickup, and 1 for shooting direction.

517 **DMC-Walker:** Shown in Fig. 7 (b), a 6 degree-of-freedom robot can locomote on a 2D plane through
518 joint motions. The agent has a 26-dimensional observation space consisting of 3 state factors: [Body
519 Position, Body Velocity, Robot Proprioception].

520 **Multi-Particle:** Shown in Fig. 7 (c), the agents are marked by small circles, while the stations are
521 marked by large circles. Only stations and agents of the same color can interact with each other. The
522 Multi-Particle environment has a 70-dimensional observation space, consisting of 20 state factors.
523 The state factors include states for each landmark and states for each agent. The action space is
524 50-dimensional, with 5 dimensions per agent that control their motions and interactions with the
525 landmarks.

526 **iGibson:** Shown in Fig. 7 (d), iGibson has 42-dimensional observation space consisting of 4 state
527 factors, including [Agent Location, Electric Appliances State, Object(s) in View, Robot Propriocep-
528 tion]. The action space is 11-dimensional, consisting of base velocity (2D), head motion (2D), arm
529 motion (6D), and gripper motion (1D).

530 D Downstream Tasks

531 DMC-Walker (Walker):

- 532 • **Run:** In this task, the walker agent is rewarded for moving forward at a particular velocity.
- 533 • **Goal Reaching:** In this downstream task, the agent has to reach randomly generated goal positions.

534 2D Gunner (2DG):

- 535 • **Unlimited Ammo (unlim):** In this downstream task, a set of targets will randomly appear, where
536 the agent needs to navigate to a position close to the target and shoot them in order to score. The
537 ammo is unlimited so the agent does not need to worry about picking up ammo.
- 538 • **Limited Ammo (lim):** This downstream task is different from the “unlimited ammo” in that the
539 agent starts with no ammo and needs to pick up ammo in order to shoot. Everything else is identical.

540 Multi-Particle (MP):

- 541 • **Sequential interaction (seq)** (easy, medium, hard): In this task, agents need to sequentially interact
542 with their corresponding station following an instruction sequence given at the start of each episode.
543 Interacting with stations in the wrong order will be penalized. The easy version of this task has a
544 sequence length of 2, while medium and hard have a sequence length of 5 and 8 respectively.
- 545 • **Food-poison (fp)** (easy, medium, hard): In this downstream task, each station will offer either
546 food or poison to the corresponding agent. Each agent needs to decide whether to interact with
547 its corresponding station based on a sequence of binary indicators provided to the agents. The
548 difficulty level has the same meaning as in the sequential interaction task.

549 iGibson (IG):

- 550 • **Look around:** In this task, the robot needs to look at objects in the room sequentially.
- 551 • **Appliances inspection:** In this task, the robot needs to navigate to different electric appliances,
552 and test whether each of them is working correctly by pointing a remote control towards it.

553 • **Housekeeping:** In this task, the robot needs to manage the electric appliances intelligently. Specifi-
554 cally, the robot needs to first look at a screen to receive instructions. Depending on the instruction,
555 the robot needs to turn on / off certain electric appliances using the remote control.

556 E Baseline Methods

557 During downstream task evaluation, we compared against the following state-of-the-art unsupervised
558 RL methods:

- 559 • **DIAYN** [12] represents skill variable z as an integer between 1 to k^N and learns skills by maximiz-
560 ing $I(\mathcal{S}; \mathcal{Z})$, the MI between \mathcal{Z} and all state factors \mathcal{S} .
- 561 • **CIC** [22] learns a state representation with contrastive learning and learns skills by maximizing
562 transition entropy in the representation space.
- 563 • **CSD** [32] learns skills maximizing distance traveled along the direction of z in the state space,
564 where distance is measured in a controllability-aware manner.
- 565 • **METRA** [33] learn a set of behaviors that collectively cover as much of the state space as possible
566 through optimizing a Wasserstein variant of the state-skill Mutual Information.
- 567 • **ICM** [34]: encourages visiting novel states by using prediction errors of action consequences as
568 intrinsic rewards.
- 569 • **RND** [4] encourages visiting novel states by using prediction errors of features computed from a
570 randomly initialized network as intrinsic rewards.
- 571 • **ELDEN** [16] operates in a factored state space similar to our approach, and encourages visiting
572 states that induce novel factor dependencies.
- 573 • **SAC** [13] where no pretraining is used, and vanilla RL is directly applied to tackle the downstream
574 tasks.

575 F Evaluating Skill Disentanglement Details

576 The DCI metric consists of three terms, namely **disentanglement**, **completeness**, and **informativeness**.
577 In the context of this work, disentanglement (\uparrow) measures, on average, to what extent each skill
578 component only affects a single state factor. Completeness score (\uparrow) measures, on average, to what
579 extent each state factor is only influenced by a single skill component. Informativeness score (\uparrow)
580 measures the repeatability of learned skills: given the skill z , how accurately we can predict which
581 states will be visited. We refer the reader to the work by Eastwood and Williams [11] for a detailed
582 discussion of these metrics and how they are calculated.

583 In the original work, measuring DCI requires knowing the ground truth generative factors. In our
584 case, the generative factors are simply the state factors, and we only need to discretize the value of
585 each state factor to make it compatible for evaluation. For each method on each domain, we collect
586 $100K$ rollout steps using the learned skill policy, $\pi(s, z)$, where the skill is (re)sampled from the
587 uniform prior distribution, $p(z)$, every 50 steps. These (state, skill) pairs are then used to calculate
588 DCI.

589 G Hyperparameters

590 **Skill Dimensions:** For all skill learning methods with discrete skills (i.e. DUSDi, DIAYN), we make
591 sure that they have equivalent capacity. Specifically, for igibson and 2D gunner, each DUSDi skill
592 consists of 3 skill components, each component with 5 possible values. As a result, DIAYN skill is an
593 integer between 1 to 125 in these two domains. The only exception is Multi-Particle, where DUSDi
594 has ten sub-skills, each with 5 possible values. Since skill as an integer between 1 and $5^{10} = 9765625$
595 is obviously challenging for DIAYN to converge, we set the number of discrete skills to be 4096 for
596 DIAYN. For continuous skills (i.e. CSD, CIC, METRA), we follow the skill dimensions specified in
597 the original papers (64D for CIC, 3D for CSD and METRA), which were shown to be effective for
598 the respective methods.

599 **Skill Learning Parameters:** All skill learning methods in our baselines use SAC to optimize for
600 the intrinsic reward, with the same policy and value network architecture. DUSDi applies additional

601 decomposition and masking to the value networks, as described in Section. 3.2, which is not applicable
 602 to the baseline methods. Due to Q-decomposition, when using the same value network architecture,
 603 DUSDi’s value network capacity is N times of the capacity of other methods’ value networks
 604 (including when comparing the variations of DUSDi, i.e., no decomposition). For a fair comparison,
 605 we also tried to increase value network capacity for other methods to match the capacity for DUSDi,
 606 but found that their skill/task learning performances do not improve significantly. This suggests
 607 (1) that, for skill learning, reward variance, rather than network capacity, is the key reason for no
 608 Q-composition variation of DUSDi to converge slowly, and (2) that, for task learning, disentangled
 609 skills, rather than network capacity, is what make DUSDi significantly outperform baselines.

610 We present the hyperparameters for SAC in Table. 2. All methods use a low-level step size of $L = 50$.

Table 2: Hyperparameters of Skill Learning.

	Name	Value
SAC	optimizer	Adam
	activation functions	ReLU
	learning rate	1×10^{-4}
	batch size	1024
	critic target τ	0.01
	MLP size	[1024, 1024]
	steps per update	2
	# of environments	4
	Temperature α	0.02
	log std bounds	[-10, 2]

611 **Downstream Hierarchical Learning:** For all skill discovery methods, downstream learning of the
 612 skill selection policy is implemented with PPO. We used the same hyperparameters for all methods
 613 across all tasks, as specified in Table. 3.

Table 3: Hyperparameters of Downstream Learning.

	Name	Value
PPO	optimizer	Adam
	activation functions	Tanh
	learning rate	1×10^{-4}
	batch size	32
	clip ratio	0.1
	MLP size	[128, 128]
	GAE λ	0.98
	target steps	250
	n steps	20
	# of environments	4
	# of low-level steps L	50

614 **Downstream Finetuning:** For all non-skill discovery methods, downstream learning is done using
 615 the same hyperparameters as pretraining (table. 2), replacing the intrinsic reward with the task reward.

616 **H Proof of Q Decomposition**

Proof.

$$\begin{aligned}
 Q_\pi(s, a, z) &= \mathbb{E}_\theta \left[\sum_{t=0}^{\infty} \gamma^t r_t \right] \\
 &= \mathbb{E}_\theta \left[\sum_{t=0}^{\infty} \gamma^t \sum_{i=1}^N q_\phi^i(z^i | s^i) - \lambda q_\psi^i(z^i | s^{-i}) \right] \\
 &= \sum_{i=1}^N \mathbb{E}_\theta \left[\sum_{t=0}^{\infty} \gamma^t (q_\phi^i(z^i | s^i) - \lambda q_\psi^i(z^i | s^{-i})) \right] \\
 &= \sum_{i=1}^N Q^i(s, a, z)
 \end{aligned}$$

617

□

618 **I Behavior Restriction of Skills via Domain Knowledge**

619 Due to the decomposable nature of the intrinsic reward of DUSDi, we can conveniently restrict the
 620 behavior of skills by constraining the skill predictor $q_\phi^i(z^i | s^i)$ for a particular state factor i . For
 621 example, if we want s^i to stay within a certain range, we can set $q_\phi^i(z^i | s^i)$ to be a uniform distribution
 622 for all s^i not within this range, effectively discouraging the agent from going out of range. In the
 623 extreme case, we can fully specify the mapping between z^i and s^i , essentially resulting in performing
 624 goal-conditioned RL for state i (as pointed out in [6]) while performing DUSDi for the rest of the
 625 state factors.

626 We qualitatively examine this idea in the iGibson domain. By restricting a mobile manipulator to only
 627 locomote in regions that are close to a whiteboard, our robot successfully learns diverse board-wiping
 628 behaviors which are otherwise extremely hard to learn. Visualizations of the learned skills can be
 629 seen at <https://sites.google.com/view/dusdi>.